CONTENTS

Supplemental Methods

Samples and magnetic resonance imaging

Patients with DSM-IV diagnoses of schizophrenia, schizophreniform or schizoaffective disorders and healthy comparison subjects from the Utrecht Schizophrenia Project and the First-Episode Schizophrenia Research Program at the University Medical Center Utrecht (sample 1[1,2,3]) and the Genetic Risk and Outcome of Psychosis (GROUP) study (sample 2[4,5]) participated after written informed consent was obtained. All subjects were between the ages of 16 and 70 years. Subjects with a major medical or neurological illness including migraine, epilepsy, hypertension, cardiac disease, diabetes mellitus, endocrine disorders, cerebrovascular disease, alcohol or other drug dependence, head trauma in the past, or an IQ below 80 were excluded. The presence or absence of psychopathological abnormality was established in all subjects using the Comprehensive Assessment of Symptoms and History[7] and Schedule for Affective Disorders and Schizophrenia Lifetime Version[8] assessed by trained and experienced psychologists and psychiatrists in the Department of Psychiatry, University Medical Center, Utrecht. All healthy comparison subjects met Research Diagnostic Criteria[9] of "never [being] mentally ill." To evaluate severity of symptoms in patients, the Positive and Negative Syndrome Scale (PANSS[10]) was performed.

Age at onset of illness was defined as the first time patients had been seeking medical or psychological help for their psychotic symptoms. Most patients (see Table 1) had received antipsychotic medication in the past and received antipsychotic medications at the time of the MRI scan. Medication included typical and atypical (clozapine, risperidone, olanzapine, or sertindole) antipsychotic agents.

The study was approved by the Medical Ethics Committee for Research in Humans (METC) of the University Medical Center Utrecht.

MRI acquisition and processing

All subjects were scanned on a 1.5 T Philips NT or Achieva scanner using the same acquisition protocol. Baseline and follow-up scans of each subject were aquired on the same scanner. Three-dimensional T1-weighted, fast field echo scans with 160 to 180 contiguous coronal slices (echo time [TE], 4.6 ms; repetition time, 30 ms; flip angle, 30°; field of view, 256 mm; $1 \times 1 \times 1.2$ mm^3 voxels) were made.

All scans were processed on the computer network of the Department of Psychiatry at the University Medical Center Utrecht. The T1-weighted images were transformed into Talairach orientation (no scaling), after which they were corrected for scanner RF-field nonuniformity with the N3 algorithm[11]. Using a partial volume segmentation technique[12] the brain was segmented into gray matter, white matter and cerebrospinal fluid. The gray matter segments were blurred using a three-dimensional Gaussian kernel (full-width half-maximum (FWHM) = 8 mm). The voxel values of these blurred segments reflect the local presence, or concentration, of gray matter and will be referred to as gray matter 'densities' (GMDs). In order to compare GMDs at the same anatomical location between all subjects, the GMD images were transformed into a standardized coordinate system using a two step process. First, the T1-weighted images were linearly transformed to a model brain[13]. In this linear step, a joint entropy mutual information metric was optimized[14]. In the second step nonlinear (elastic) transformations were calculated to register the

linearly transformed images to the model brain up to a scale of 4 mm (FWHM), thus removing global shape differences between the brains, but retaining local differences (ANIMAL[15]). The GMD maps were now transformed to the model space by applying the concatenated linear and nonlinear transformations. Since the density maps have been blurred to an effective resolution of 8 mm, it is not necessary to keep this information at the 1-mm level. Therefore, the maps were resampled to voxels of size $2 \times 2 \times 2.4$ mm^3, i.e., doubling the original voxel sizes. These resampled GMD maps were used as feature vectors for the SVM/SVR analyses.

For further details on the samples and MRI processing we refer to[1,2,3,4,5,6].

Brain-age model (M_{BA})

The brain-age model (M_{BA}), was built on all HC baseline GMD images (N=386). A support vector regression (SVR) machine was trained to predict a subject's chronological age from the GMD values in that subject's image. In a formula:

$$M_{BA}(x) = w_{BA} \cdot x + b_{BA} \quad (1),$$

where x is the subject's feature vector, containing the GMD values of all voxels within the intracranial mask; w_{BA} and b_{BA} are the model's weight vector and offset respectively. During the training phase of the model, their values are optimized to yield the best age predictions, i.e. $M_{BA}(x) \approx$ age, for all subjects. The model's performance is assessed by the amount of chronological age variance explained by the predicted age (R-squared (R^2)) and the mean absolute error (MAE) between predicted and chronological age. Following earlier works[16,17], the predicted age will be called the brain-age (BA) and its deviation from the chronological, or true, age, the brain-age gap[16]:

$$G_{BA} = BA - age \quad (2).$$

The brain-age gap, G_{BA}, reflects whether a subject's brain appears older or younger than expected from its age.

When applied to a follow-up scan of the same subject at age', the model predicts a brain-age BA' and we can calculate the brain-age gap $G'_{BA} = BA' - age'$. The change in BA is $\Delta BA = BA' - BA$, and the change in G_{BA} is $\Delta G_{BA} = G'_{BA} - G_{BA}$. The (annual) rates of change are: $\Delta G_{BA}/\Delta age = \Delta BA/\Delta age - 1$, with $\Delta age = age' - age$, the scan interval. While $\Delta BA/\Delta age$ reflects the relative aging speed of the brain, $\Delta G_{BA}/\Delta age$ provides the excess brain aging speed, telling whether the brain is aging progressively or regressively. We will call $\Delta G_{BA}/\Delta age$ the brain age acceleration rate.

The model's performance is tested both in the training phase (goodness of fit) and in the test phase, using leave-one-out (LOO) cross-validation. During this phase, each subject is subsequently left out of the sample. The SVR is trained on the remaining N-1 subjects and the resulting model is applied to the subject that was left out, predicting this subject's (brain)age. If a subject's follow-up (brain-)age has to be predicted, the brain-age model that was built leaving out this subjects' baseline image was applied.

The weight vector w_{BA} describes the GMD pattern of the aging brain. Positive and negative values reflect in which locations (voxels) in the brain increasing or decreasing GMD contributes to predicting an older age, respectively. The larger the absolute value of a voxel's w_{BA}, the more important it is for predicting age.

A subject's GMD pattern can be decomposed into a part coinciding with the aging pattern and the remaining part, perpendicular to it. This is done by projecting the subject's feature vector x on to the weight vector w_{BA}:

$x = x_{//BA} + x_{\perp BA}$, with

$x_{//BA} = (x \cdot w_{BA}/||w_{BA}||)w_{BA}$, and (3)

$x_{\perp BA} = x - x_{//BA}$.

The brain-age gap in terms of GMD is then:

$G_{xBA} = x_{//BA} - x_{//age} = G_{BA} / ||w_{BA}||$ (4).

This decomposition allows us to represent the brain-age (gap) in terms of gray matter densities. We will call $x_{//BA}$ the subject's neuroanatomical fingerprint of his/her brain-age, and G_{xBA} the fingerprint of his/her brain-age gap. Via G_{xBA} the brain-age gap and changes in it can be compared to (changes in) other measures, such as the size of the GMD differences between subjects along the HC/SZ discrimination pattern (the SZ fingerprint; see next section).

SVR parameter optimization

Two parameters, the complexity parameter C and the sparsity parameter ν, need to be specified for SVR. Since it has been shown (Franke et al, 2010) that tuning these parameters can increase the model's performance, a grid search in the (C, ν) parameter space was carried out to find the optimal settings. R-squared (R^2), the fraction of variance in age explained by the model in a cross-validation (LOO) loop, was used as measure of performance. The figure below shows the results. There is a plateau in performance for C>0.0001 and ν>0.1, where all combinations of C and ν yield the same performance of R^2=0.79. Apparently, in this part of parameter space we have reached a stable model that is not further dependent on changes in C or ν. We chose ν=0.5 and C=0.01 for our model.

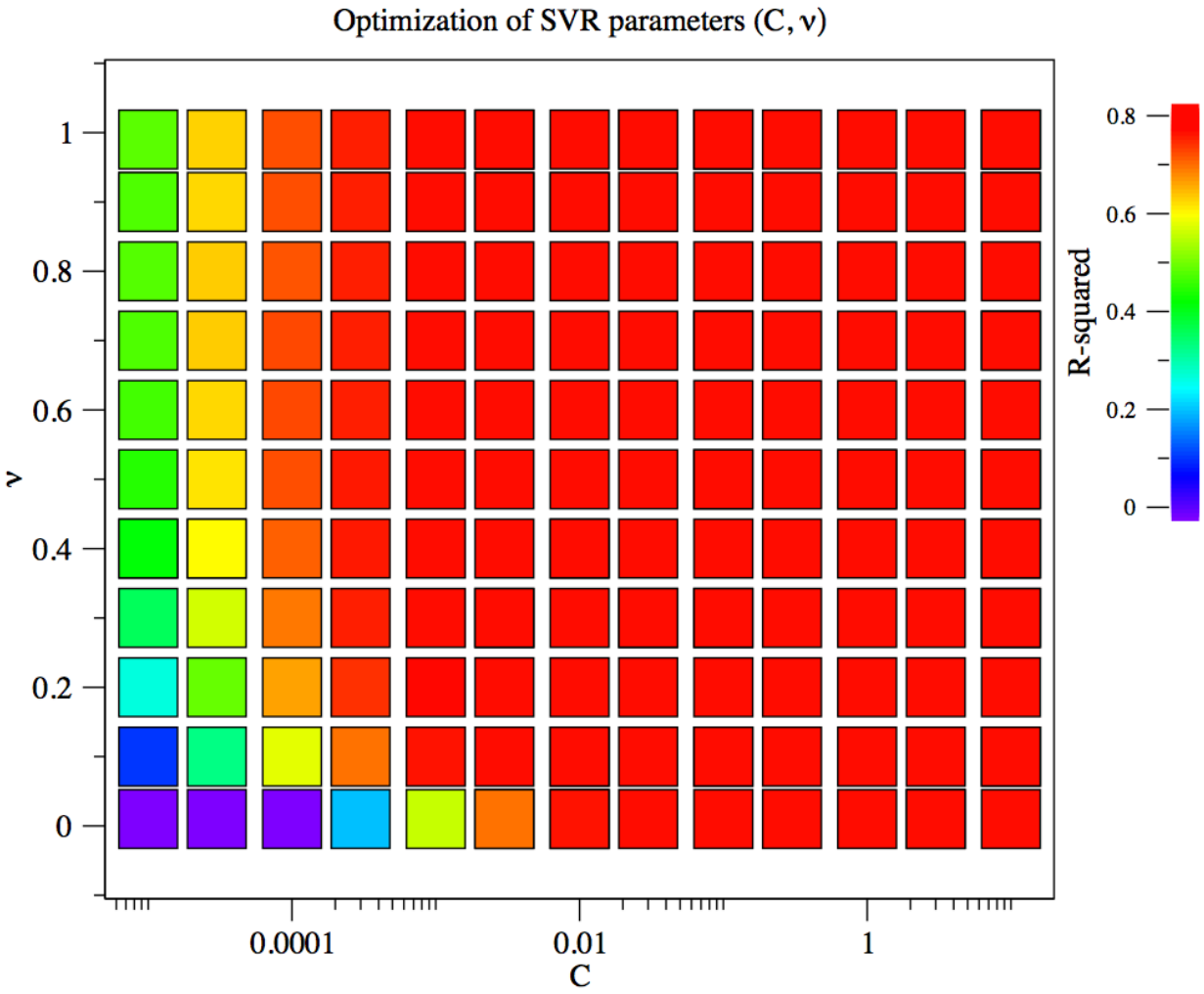

For an unbiased estimation of the generalizability of our brain-age model we also carried out a nested cross-validation procedure. This double cross-validation consisted of an outer and inner loop. For the outer loop the sample of healthy baseline images was split into 20 partitions which were subsequently held back to validate the age prediction model built in the inner loop. In the inner loop the age prediction model was optimized with respect to the parameters ν and C using a leave-one-out cross-validation procedure. The procedure yielded no significantly different results as compared to the grid search: (ν=0.5,C=0.01) lay in a part of the parameter space with accuracies closely around the one found from the grid search: 0.791+0.010. Optimal prediction accuracy from the nested cross-validation procedure was 0.798, thus somewhat higher than our reported value.

HC-SZ Classification model

A classification model was built following the same procedures as published before[18,19]. A support vector machine (SVM) was trained to predict patient status (y_{SZ}=1: SZ, y_{SZ}=-1: HC) from a subject's GMD image (feature vector x). In a formula:

$$y_{SZ} = M_{SZ}(x) = w_{SZ} \cdot x + b_{SZ} \quad (5),$$

where w_{SZ} and b_{SZ} are again the model's weight vector and offset, respectively. During the training phase their values are optimized to give the best possible prediction of y_{SZ}. In the LOO cross-validation phase, the model's performance is tested by assessing the percentages of correctly classified subjects: sensitivity = number of true positives / number of patients; specificity = number of true negatives / number of healthy subjects; total accuracy = number of correctly classified subjects / total number of subjects. (See[18] for details on LOO.)

The weight vector w_{SZ} can be used to split the feature vector x in a part coinciding with the weight vector and the part perpendicular to it:

$x = x_{//SZ} + x_{\perp SZ}$, with

$$x_{//SZ} = (x \cdot w_{SZ}/||w_{SZ}||)w_{SZ}, \text{ and} \quad (6)$$

$x_{\perp SZ} = x - x_{//SZ}$.

Taking the mean y_{SZ} value of the healthy subjects from the LOO procedure as the healthy reference value, $\langle y_{SZ} \rangle_{HC}$, we can calculate a subject's "SZ gap" by subtracting this value from the subject's y_{SZ}:

$$G_{SZ} = y_{SZ} - \langle y_{SZ} \rangle_{HC} \quad (7a).$$

However, since the values of y have no absolute meaning, it is more useful to calculate this gap in terms of GM densities. Dividing eq. (7a) by the length of w_{sz}, $||w_{SZ}||$, gives:

$$G_{xSZ} = x_{//SZ} - \langle x_{//SZ} \rangle_{HC} \quad (7b),$$

which will be referred to as the SZ fingerprint of the brain. It may be directly compared to the brain-age gap on the same scale (eq. 4).

A rererence model was built from 'raw' GMD images, uncorrected for age, gender and handedness. Then a model was built from GMD images corrected for brain-age, i.e. using the component of the GMD pattern not coinciding with the brain-age pattern ($x_{\perp BA}$ in eq. 3).

Comparing and combining outputs from different models using fingerprints

The brain-age gap, G_{BA}, can be used to split HCs from SZs using a threshold gap value, i.e., if a subject's G_{BA} exceeds this G_{BA}-threshold, then this subjects will be classified as SZ patient, otherwise as HC subject.

The representation of brain-age gap and schizophrenia gap in terms of GMD fingerprints (eqs. 4 and 7b) allows us to compare them statistically and to use them together as features in a linear SVM, to separate HC and SZ subjects. The resulting decision function is:

$$y = w_1 G_{xBA} + w_2 G_{xSZ} + b \quad (8),$$

where subjects with $y>0$ will be classified as SZ and if $y<0$ as HC. The weights w_1 and w_2 reflect the relative importance of the brain-age gap and SZ gap, respectively.

Visualization of the accelerated aging in schizophrenia

To illustrate that the progressive increase in brain-age gap in SZ truly reflects changes in GMD that are qualitatively the same as those in healthy aging – but at an augmented pace, we test whether the changes in GMD with time in HC subjects can be scaled using a single scaling factor (>1) to obtain the GMD changes with time in SZ patients. This scaling, formally an accelerated increase of the length of the brain-age fingerprint ($||x_{//BA}||$), will be visualized in the brain areas most prominently related to aging. These main regions of interest (ROI) of the neuroanatomical pattern related to aging were found by selecting the voxels with $|w| \geq 0.00050$ from weight map w_{BA}, while setting a lower limit of size at 100 voxels or more. This resulted in 24 main ROIs, consisting of 2.4% of the features, but representing 8.0% of the summed absolute weights. The mean rate of change in GMD in each ROI was calculated for all subjects and averaged per group (HC, SZ). To determine the relationship between the rate patterns of the two groups, robust regression with Tukey's biweight function[20] was used. Robust regression is, in contrast to standard least squares fitting, less sensitive to outliers in the data, caused by ROIs involved in both the aging and the SZ-specific pattern. To find the scaling factor that best fitted the HC rates (R_{HC}) to the SZ rates (R_{SZ}) for all ROIs simultaneously, first a full linear fit was tried: $R_{SZ} = A \times R_{HC} + B$, with A the acceleration factor in SZ and B an offset, independent of the HC aging pattern. If the offset (B) was not significantly different from zero, it was dropped from the fitting procedure and the pure acceleration factor A in SZ was calculated.

Methodological Considerations

Our brain-age model is based on the features that are the default output from our image processing pipeline (1), making it possible to relate the machine learning results to published group-statistical results, in particular those related to progressive brain changes (2,3,5). Although a full, technical, investigation of brain-age methodology falls beyond the scope of this work, the difference between the brain-age gap in SZ patients found by us (3.4 year) as compared to that of the only other study that investigated brain-age in SZ (17) (5.5 year) should be viewed in light of differences in sample and image acquisition and methodology. Our features are the set of all voxels in which gray matter density was measured, which had been smoothed with an 8-mm 3D Gaussian kernel, nonlinearly transformed to a template, and resampled to a resolution of $2 \times 2 \times 2.4$ mm^3. The choice to use gray matter (density) was made because of the abundant evidence of (group) differences between SZ patients and HC subjects; moreover, GMDs processed this way were also the basis of our previous machine learning studies on schizophrenia (18,19). The following choices regarding further processing of GMD could be made: the use of GM densities

or volumes; smoothing (with different kernel widths) or not; linear (affine) or nonlinear transformations; resampling (to different voxel resolutions) or not; feature reduction or not. The choices that are expected to be of most influence are (i) GM densities or volumes and (ii) feature reduction or not. We thus built the following models:

M1: M_{BA}(GMD|smooth|nonlin|resa), i.e. the brain-age model M_{BA} in our study

M2: M_{BA}(GMD|smooth|nonlin|resa|pca), i.e. M_{BA}, but using the scores on the principal components (feature reduction)

M3: M_{BA}(GMV|nonlin|resa), i.e. based on (unsmoothed) GM volumes instead of densities

M4: M_{BA}(GMV|nonlin|resa|pca), i.e. M3, but using the scores on the principal components (feature reduction)

In order to come as close as possible to the approach of Koutsouleris et al, who combined PCA scores of affinely transformed GMDs and PCA scores of nonlinearly transformed GM volumes (unsmoothed), we also built:

M5: M_{BA}(GMD|affine|resa|pca $\oplus$ GMV|nonlinear|resa|pca)

The image processing steps were carried out using our standard tools (MNI minc tools and in-house developed software); the principal component analysis was done in Matlab). Parameters were optimized as before, including, for the models involving PCA, the number of components.

The performance of the models was assessed, again, by calculating mean absolute error (MAE) and R^2. The results:

Brain-age model	#features	MAE (year)	R^2
M1 = ref.	157256	4.31	0.791
M2	200	4.76	0.750
M3	157256	5.22	0.695
M4	150	5.50	0.666
M5	300	4.92	0.726

The reference model, the brain-age model of our study, clearly outperforms the other models on both MAE and R^2. The models based on GMV only (M3 and M4) perform poorest. Brain-age gaps were 3.4 year for M2, the same as for M1, 2.9 year for M3, 4.5 year for M4, and 4.6 year for M5. Although different baseline brain-age gaps are thus found, this variation concurs with variations in performance. For our training sample and MRI acquisition, the set of unreduced GMDs appears to produce the best age predictions in terms of MAE and R^2.

Reverse brain-age modeling

To illustrate the fact that the brain-age model is really picking up the chronological aging of the brain in healthy subjects and an accelerated, but normal, aging in schizophrenia patients, we did the reverse experiment: We built a brain-age model on the set of baseline scans of the SZ patients (N=341), and applied this model to the scans of the healthy subjects (N=386). The

performance of the SZ-based brain-age model was assessed, again, by measuring the mean absolute error (MAE) and R^2. Results: MAE = 4.36 year, very comparable to M_{BA}'s (4.31 year); the fraction of explained variance in age = 0.70, somewhat lower than that of M_{BA} (0.79).). The mean brain-age gap was $G_{BA}(SZ)$ = 0.0145 year = 5 days, so, about zero. Application of the SZ-based brain-age model to the healthy subjects yielded a mean brain-age gap of $G_{BA}(HC)$ = -4.83 year. The predicted age of the controls is lower than the true age, indicating that the brains of the controls appear about 4.8 years younger than they really are –from the point of view of the ill-brain-age model. Although of the right sign and order of magnitude, the fact that it is about 40% larger than the gap of SZ patients found by the normal brain-age model (3.36 year), might seem surprising at first sight. There is, however, a simple explanation for it. In the presence of non-age-related progressive brain changes, that is, brain changes that increase with time (thus age) but are non-specific for healthy aging, the SZ-based brain-age model will be fooled: it will interpret the age-related changes as (normal) aging: a higher age will be predicted based on both the healthy-aging and the ill-aging patterns in the brain; the predicted age in healthy individuals will thus be lowered by both the absence of accelerated aging and the absence of disease-related progressive brain changes. Note that application of the normal brain-age model to SZ patients does not have this "problem", since the patterns of healthy aging and ill-aging are, by definition, orthogonal.

Supplemental Results

Visualization of the accelerated aging pattern in schizophrenia

The 24 main ROIs of the neuroanatomical pattern related to aging are listed in Table S2. The ROIs have been sorted according to decreasing size and sign of the weights (1–17, negative; 18–24, positive). Figure S1 shows their locations. Figure S2 shows the mean annual GMD change rates for HC and SZ subjects. The fitting procedure indicated that there was no significant offset (B=-0.00031; t=0.96; p=0.3) and that the SZ pattern was a scaled version of the HC pattern with scaling factor A=1.29 (t=9.63; p<0.0001), close to the 1.36 year/year found from the full brain-age model. SZ and HC had very different rates in ROI 12: the left occipital pole, which also was part of the SZ pattern.

TABLE S1. Mean (SD) output values of predictors in GMD space

Model / group:	baseline		follow-up		change	
	mean(sd)	dif / t	mean(sd)	dif / t	mean(sd)	dif / t
BA -HC:	.047 (.976)	.501 / 4.59*	-.021 (1.034)	.652 / 5.39*	-.068 (.481)	.151 / 2.35†
-SZ:	.548 (.978)		.631 (1.120)		.083 (.639)	
SZ -HC:	-.329 (.585)	.496 / 7.54*	.094 (1.237)	.628 / 3.73#	.423 (1.261)	.132 / .77
-SZ:	.167 (.592)		.722 (1.686)		.555 (1.718)	

'dif' refers to SZ minus HC (with t-value); 'change' refers to follow-up minus baseline; *p<0.00001; #p<0.001; †p<0.01. Information in this table is for subjects with a baseline and follow-up scan.

TABLE S2. Main ROIs of the brain-age pattern

index	w(mean)	size	side	structure
1	-0.690	269	L	Inferior temporal gyrus
2	-0.609	236	R	Superior occipitofrontal fasciculus
3	-0.613	204	R	Middle frontal gyrus
4	-0.642	185	L	Cerebellum, tuber/declive of vermis
5	-0.661	184	R	Angular gyrus
6	-0.668	167	R	Cuneus
7	-0.676	145	R	Caudate
8	-0.682	143	R	Cingulate gyrus
9	-0.663	133	L	Middle frontal gyrus
10	-0.670	126	L	Superior occipitofrontal fasciculus
11	-0.638	118	L	Superior longitudinal fasciculus
12	-0.660	115	L	Occipital pole
13	-0.625	115	L	Superior temporal gyrus
14	-0.580	113	R	Middle cerebellar pedunculus
15	-0.606	111	R	Superior temporal gyrus / temporal plane
16	-0.659	110	R	Superior frontal gyrus
17	-0.612	100	R	Lingual gyrus
18	0.766	237	L	Thalamus
19	0.765	210	R	Thalamus
20	0.648	210	L	Middle temporal gyrus
21	0.743	177	-	Cisterne laminae tecti/venae cerebri magnae
22	0.557	164	-	Aquaduct/fourth ventricle
23	0.623	140	L	Inferior parietal lobule
24	0.598	119	L	Angular gyrus

ROIs sorted by size (number of voxels) for negative (index 1-17) and positive (index 18-24) separately. W(mean) is the mean value ($\times$1000) of the weights from weight map w_{BA} in the ROI. L=left, R=right. See Figure S1 for the locations by index.

TABLE S3. Associations between clinical parameters and BA/SZ gap (changes)

		G_{BA} G_{SZ} (df) (baseline)	G_{BA} G_{SZ} (df) (follow-up)	$\Delta G_{BA}/\Delta age$ $\Delta G_{SZ}/\Delta age$ (df) (acceleration rate)
PANSS Total	baseline	-0.20 -1.75 (202)		1.98 0.48 (113)
GAF	,,	-0.15 - 1.40 (110)		-0.72 -2.08 (50)
PANSS Total	follow-up		1.10 -0.59 (145)	**3.44** 0.41 (145)
GAF	,,		**-3.49** -0.85 (118)	**-3.31** -1.93 (118)
hospitalizations #	/interval			**5.88** 2.36 (129)
hospitalizations dur.	/interval			**3.76** 2.50 (128)
cum. antipsychotics	/interval			**3.31** **4.89** (68)
antipsychotics dose	follow-up		**3.33** 1.61 (93)	1.95 0.41 (93)

t-values (degrees of freedom (df)) of the association between G_{BA}, G_{SZ} and their change rates, and a number of clinical parameters: PANSS Total and GAF scores; number of hospitalizations (#), hospitalization duration and cumulative antipsychotics dose, all divided by the scan interval, and antipsychotics dose at follow-up. Bold values are significant after Bonferroni-correction for multiple comparisons (i.e., at $p<0.0025$).

FIGURE S1. Design of the study: Use of the different (sub)samples

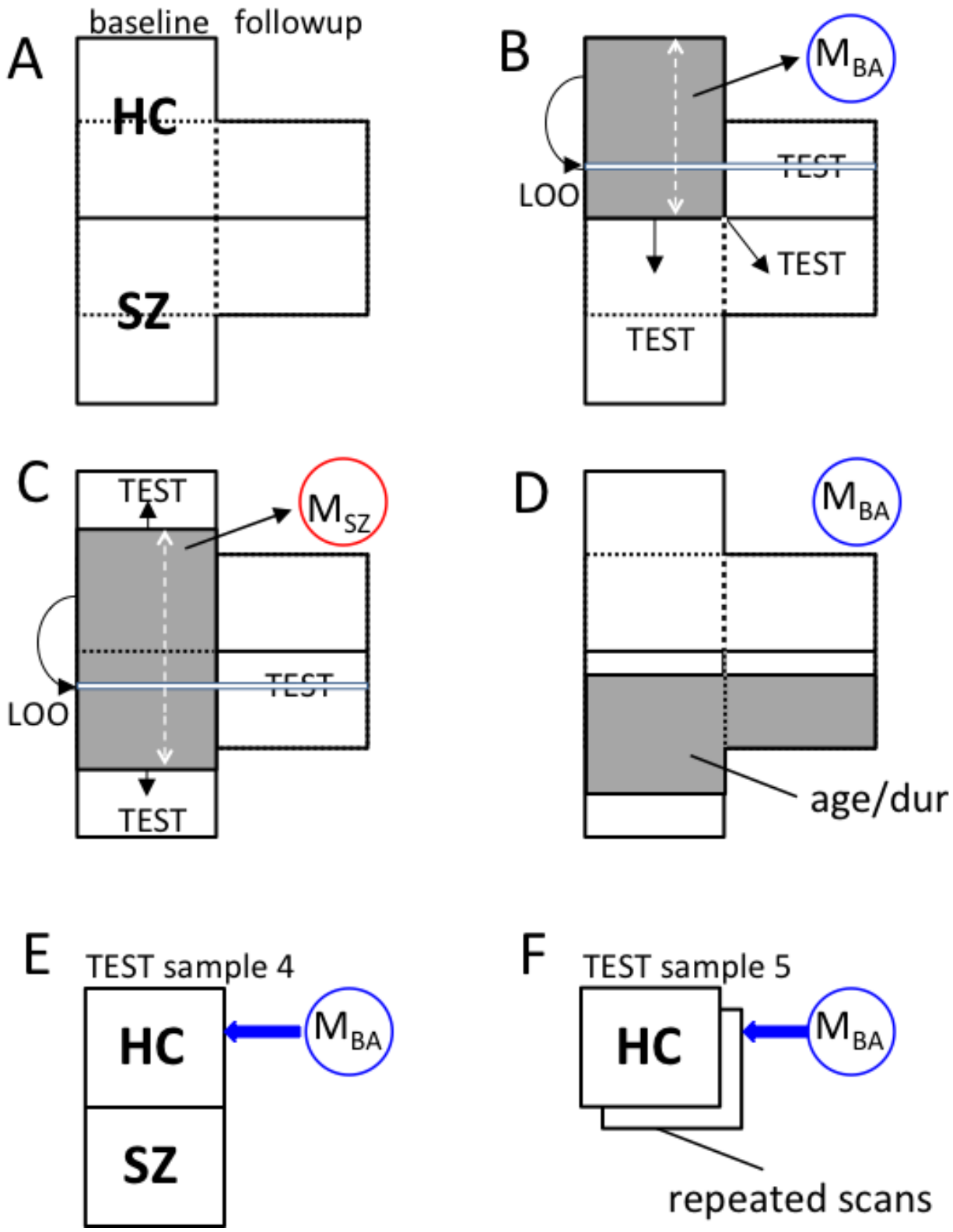

(A) The main sample (samples 1, 2 and 3, combined – see Methods) consists of baseline scans (left column) and follow-up scans (right column) and includes healthy control (HC) subjects (upper part); and schizophrenia patients (SZ; lower part). The horizontal dashed lines divide the subjects into a part that has one or more follow-up scans and a part that does not have any follow-up scan.

(B) The brain-age model (M_{BA}) is trained on the healthy control baseline scans (gray area). The performance of the model is tested within the training sample by leave-one-out (LOO) cross-validation. The horizontal white line indicates the left-out subject; the vertical dashed white arrow reflects that each of the training subjects is subsequently left out during the LOO operation. The model is also tested (TEST) the training subjects' follow-up scans (with the baseline scan of a tested subject left-out, as indicated by the extension of the white line into the follow-up sample) and applied to independent subjects: the schizophrenia baseline and follow-up scans.

(C) The schizophrenia model (M_{SZ}) is trained on a subsample of matched healthy control (N=267) and schizophrenia (N=274) baseline scans (gray area). The performance of the model is applied in the baseline scans using leave-one-out (LOO) cross-validation within the training sample and to the unused baseline subjects (TEST). The model is also applied to the follow-up scans (with, again, the baseline scan of a tested subject left-out, as indicated by the extension of the white line into the follow-up sample).

(D) The analysis of the influence of age and duration of illness on the brain-age gap in schizophrenia patients (see Figure 2) is carried out in all baseline and follow-up scans of schizophrenia patients for whom this information is available (gray area).

(E) The validity of the brain-age model (M_{BA}) is tested in an independent sample 4 including healthy subjects and schizophrenia patients scanned at 3 tesla.

(F) The reliability of the brain-age model (M_{BA}) is tested in an independent sample 5 including five healthy volunteers scanned twice within a short period of time.

FIGURE S2.

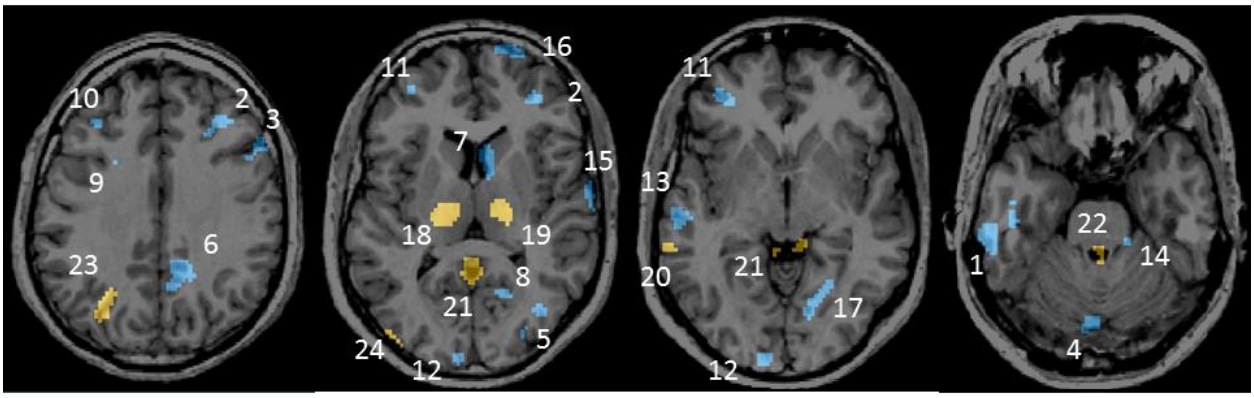

Locations of the 24 main ROIs of the brain-age pattern (see Table S2) in four axial slices of the brain. ROIs in which a lower GMD leads to a younger age prediction are shown in blue, whereas ROIs in which a higher GMD leads to an older age prediction are shown in yellow. Each ROI is labeled with its index (Table S2). Note that most regions are much larger than the part visible in these slices.

FIGURE S3.

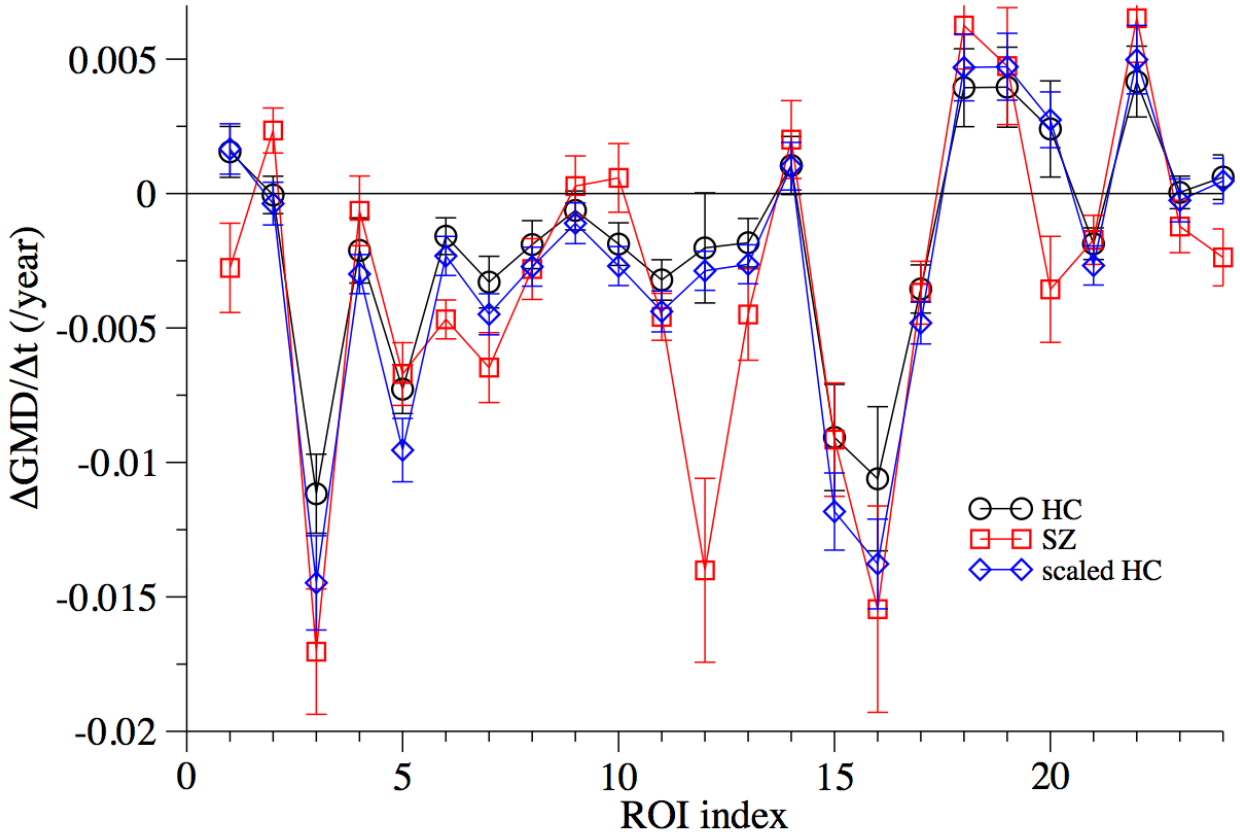

Mean annual changes in GMD (R = ΔGMD/Δt) in the 24 main ROIs of the brain-age pattern (see Table S2 and Figure S2), for healthy subjects (HC, black circles) and schizophrenia patients (SZ, red squares). The pattern for SZ is best matched by a scaled version of the HC pattern: $R_{SZ} = 1.29 \times R_{HC}$. The proportion of explained variance of 0.81 is calculated without the ROI (no. 12) that is shared with the SZ prediction pattern (see Results section).

FIGURE S4.

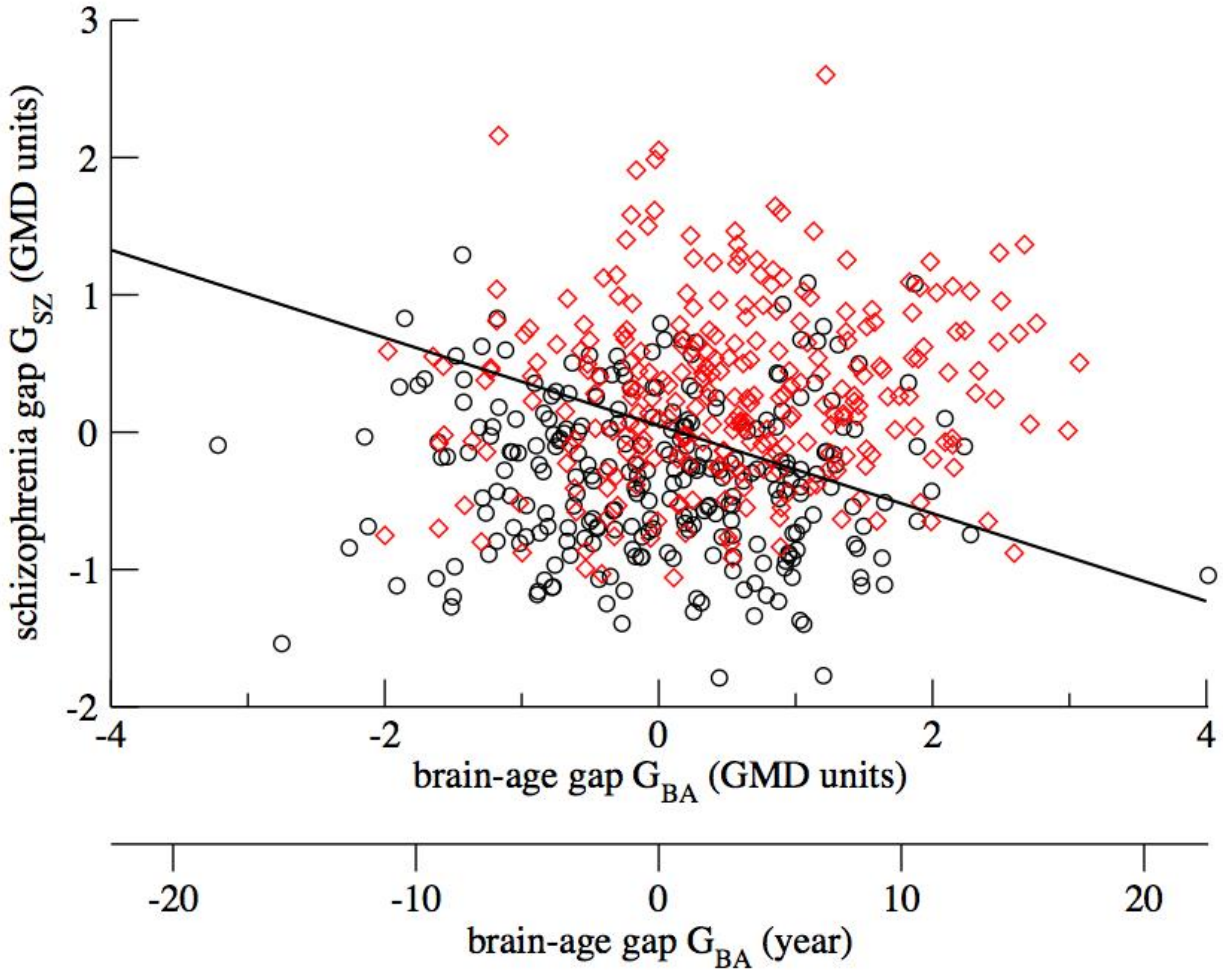

Separation of HC and SZ subjects by a linear SVM using brain-age gap and schizophrenia gap information in GMD space. Applying a G_{BA} = 1.55 year threshold value, GBA can be used to separate HCs and SZs with an accuracy of 60.2% (sensitivity 59.5%, specificity 60.9%). The performance at follow-up, with the same threshold, did not change significantly. Training a two-feature SVM on the (x_{BA}, x_{SZ}) data resulted in a HC/SZ classification model with 71.5% accuracy. At follow-up this accuracy was 64.1%. Weight values were 0.50 (brain-age) and 1.57 (SZ), indicating a larger weight for the SZ feature. At follow-up the weight values were 0.59 and 0.36, respectively. The relative importance of brain-age in the classification of SZ has increased.

Supplemental References

1. Hulshoff Pol HE, Schnack HG, Mandl RC, van Haren NE, Koning H, Collins DL, Evans AC, Kahn RS (2001). Focal gray matter density changes in schizophrenia. Arch Gen Psychiatry 58:1118-1125.

2. Van Haren NE, Hulshoff Pol HE, Schnack HG, Cahn W, Mandl RC, Collins DL, Evans AC, Kahn RS (2007). Focal gray matter changes in schizophrenia across the course of the illness: a 5-year follow-up study. Neuropsychopharmacology 32:2057-2066.

3. Cahn W, Hulshoff Pol HE, Lems EB, van Haren NE, Schnack HG, van der Linden JA, Schothorst PF, van Engeland H, Kahn RS (2002). Brain volume changes in first-episode schizophrenia: a 1-year follow-up study. Arch Gen Psychiatry 59:1002-1010.

4. Boos HB, Cahn W, van Haren NE, Derks EM, Brouwer RM, Schnack HG, Hulshoff Pol HE, Kahn RS (2012). Focal and global brain measurements in siblings of patients with schizophrenia. Schizophr Bull 38:814-825.

5. Kubota M, Haijma S, Schnack H, Cahn W, Hulshoff Pol HE, van Haren NE, Kahn RS. Progressive brain changes are related to IQ change in schizophrenia. JAMA Psychiatry (in press).

6. Van der Schot AC, Vonk R, Brouwer RM, van Baal GC, Brans RG, van Haren NE, Schnack HG, Boomsma DI, Nolen WA, Hulshoff Pol HE, Kahn RS (2010). Genetic and environmental influences on focal brain density in bipolar disorder. Brain 133:3080-3092.

7. Andreasen NC, Flaum M, Arndt S (1992). The Comprehensive Assessment of Symptoms and History (CASH): an instrument for assessing diagnosis and psychopathology. Arch Gen Psychiatry 49:615-623.

8. Endicott J, Spitzer RL (1978). A diagnostic interview: the Schedule for Affective Disorders and Schizophrenia. Arch Gen Psychiatry 35:837-844.

9. Spitzer RL, Endicott J, Robins E (1978). Research Diagnostic Criteria: rationale and reliability. Arch Gen Psychiatry 35:773-782.

10. Kay SR, Fiszbein A, Opler LA (1987). The positive and negative syndrome scale (PANSS) for schizophrenia. Schizophr Bull 13:261-276.

11. Sled JG, Zijdenbos AP, Evans AC (1998). A nonparametric method for automatic correction of intensity nonuniformity in MRI data. IEEE Trans Med Imaging 17:87- 97.

12. Brouwer RM, Hulshoff Pol HE, Schnack HG (2010). Segmentation of MRI brain scans using non-uniform partial volume densities. Neuroimage 49:467-477.

13. Hulshoff Pol HE, Schnack HG, Mandl RC, van Haren NE, Koning H, Collins DL, Evans AC, Kahn RS (2001). Focal gray matter density changes in schizophrenia. Arch Gen Psychiatry 58:1118-1125.

14. Maes F, Collignon A, Vandermeulen D, Marchal G, Suetens P (1997). Multimodality image registration by maximization of mutual information. IEEE Trans Med Imaging 16:187-198.

15. Collins DL, Holmes CJ, Peters TM, Evans AC (1996). Automatic 3-D model-based neuroanatomical segmentation. Hum Brain Mapp 4:190-208.

16. Franke K, Ziegler G, Klöppel S, Gaser C; Alzheimer's Disease Neuroimaging Initiative (2010). Estimating the age of healthy subjects from T1-weighted MRI scans using kernel methods: exploring the influence of various parameters. Neuroimage 50:883-892

17. Koutsouleris N, Davatzikos C, Borgwardt S, Gaser C, Bottlender R, Frodl T, Falkai P, Riecher-Rössler A, Möller HJ, Reiser M, Pantelis C, Meisenzahl E (2014). Accelerated brain aging in schizophrenia and beyond: a neuroanatomical marker of psychiatric disorders. Schizophr Bull 40:1140-1153.

18. Nieuwenhuis M, van Haren NE, Hulshoff Pol HE, Cahn W, Kahn RS, Schnack HG (2012). Classification of schizophrenia patients and healthy controls from structural MRI scans in two large independent samples. Neuroimage 61:606–612.

19. Schnack HG, Nieuwenhuis M, van Haren NE, Abramovic L, Scheewe TW, Brouwer RM, Hulshoff Pol HE, Kahn RS (2014). Can structural MRI aid in clinical classification? A machine learning study in two independent samples of patients with schizophrenia, bipolar disorder and healthy subjects. Neuroimage 84:299-306.

20. Fox J (1997). Applied regression analysis, linear models, and related models. Sage publications, Inc.